

## Four micron infrared observations of the comet Shoemaker-Levy 9 collision with Jupiter at the Zelenchuk Observatory: Spectral evidence for a stratospheric haze and determination of its physical properties

J. Rosenqvist,<sup>1</sup> Y.G. Biraud,<sup>1</sup> M. Cuisenier,<sup>1</sup> A. Marten,<sup>1</sup> T. Hidayat,<sup>1</sup> G. Chountonov,<sup>2</sup> D. Moreau,<sup>3</sup> C. Muller,<sup>3</sup> I. Maslov,<sup>4</sup> M. Ackerman,<sup>3</sup> Y. Balega,<sup>2</sup> O. Korablev,<sup>4</sup>

**Abstract.** We present preliminary results derived from low spectral resolution infrared spectra of the comet impact sites onto Jupiter. Fragments W/K were tracked several days after the collision at the SAO 6m-telescope on July 22 and 27. A systematic increase of the spectral radiance is observed for fragment W/K spectra as compared to undisturbed region spectra. This change is interpreted as the evidence for a stratospheric haze produced by the collision. From the spectral shape of this relative increase, the albedo of the haze can reach values as low as 0.06 but is constrained between 0.13 and 0.15 if the spot size is 3". No stringent constraint is obtained for the altitude of this haze even if a 5-50 mbar level seems to be possibly the best estimate. The particles in the haze should play a significant role in the thermal balance over impact sites. The fragments W/K spectra between July 22 and July 27 show a high stability of the haze between both dates.

### Observations

The recent dramatic collision of comet Shoemaker-Levy 9 into the Jovian atmosphere in July 1994 provided an exceptionally huge amount of data of all kinds. Several months after the impacts of SL-9 fragments, it is useful to present some preliminary results so that an understanding of the physical processes which govern such an event can emerge. In this spirit, we present a progress report inferred from observations performed at low spectral resolution (7-15 cm<sup>-1</sup>) in the 4 μm spectral range. The spectrometer we used is a classical rapid scanning Michelson interferometer installed at the Nasmyth cabin of the alt-azimuthal 6m-telescope of the Special Astronomical Observatory of Zelenchuk (Cau-

casus/Russia). The detector is an InSb 2×2 mm square detector operating at 77K. Our July program is part of a long-term cooperation concerning planet and aeronomy observations using a Fourier spectrometer able to work between 3 and 12 μm at a maximum resolution of 0.1 cm<sup>-1</sup>. An unpredictable technical problem forced us to work only at low spectral resolution between 7 and 15 cm<sup>-1</sup> depending on the spectrum. In order to get a somewhat homogeneous set of spectra, we have decided to degrade the spectral resolution down to the lowest resolution of 15 cm<sup>-1</sup>.

The SL-9 impact sites onto Jupiter were observed on July 16, 17, 22, and 27 only. Spectra of impacts K and W were recorded in the 2450-2750 cm<sup>-1</sup> range. The circular aperture was 5" in diameter. Because of very poor weather conditions and lack of time, the observation of a star at the same elevation as Jupiter was not performed during the same days. In our spectral range, essentially two N<sub>2</sub>O bands are responsible for the terrestrial absorption. Because the lack of accurate absolute calibration, we were obliged to work on the relative variation of a spectrum without spot compared to a spectrum containing the fragments W/K couple. This variation can be interpreted as the relative difference spectrum due to the presence of the fragments W/K in the field of view of the instrument. It is defined as:

$$\frac{\text{Spec with spot}(\nu) - \text{Spec without spot}(\nu)}{\text{Spec without spot}(\nu)} \times 100 \% \quad (1)$$

The spectral influence of the N<sub>2</sub>O telluric features on our Jovian spectra is minor because of the effective low spectral resolution. Figure 1 shows an observed original spectrum which has been arbitrarily rescaled at 2580 cm<sup>-1</sup> with a synthetic spectrum convolved at 7cm<sup>-1</sup>. The presence of the expected methane bands is almost certain though some patterns remain unexplained. This observed spectrum has been obtained with the highest spectral resolution of 7 cm<sup>-1</sup>.

### Results

Typical relative variations of spectra are presented in Fig. 2. Two classes of relative spectra are clearly shown depending on the presence or absence of impact site in the field of view of the instrument. Moreover, the sta-

<sup>1</sup> DESPA, Observatoire de Paris-Meudon

<sup>2</sup> Special Astrophysical Observatory, Zelenchuk

<sup>3</sup> Institut d'Aéronomie Spatiale, Brussels

<sup>4</sup> IKI, Moscow

Copyright 1995 by the American Geophysical Union.

Paper number 95GL00950

0094-8534/95/95GL-00950\$03.00

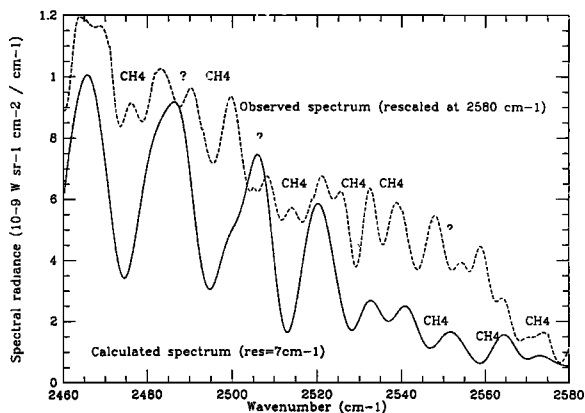


**Figure 1.** Comparison between a spectrum measured at the impact location W+K and a calculated undisturbed spectrum of Jupiter (without influence of SL9 impacts).

bility of the spectrum corresponding to the W/K site between July 22 and 27 is remarkable. The fact that the two existing classes are easily differentiated led us to be confident with the relative scale of the variation. In order to explain the relative variation of the spectra, we have used a complete line-by-line radiative transfer model derived from Marten *et al.* (1994a) in the 2450–2600  $\text{cm}^{-1}$  spectral range. We will extend the model to 2750  $\text{cm}^{-1}$  in the future. The  $\text{H}_2$ - $\text{H}_2$ ,  $\text{H}_2$ -He pressure-induced absorption,  $\text{NH}_3$ ,  $\text{PH}_3$ ,  $\text{H}_2\text{O}$  and  $\text{CH}_4$  opacities were accounted for. The thermal profile was taken from Orton *et al.* (1992). The frequency step of the synthetic calculation is 0.01  $\text{cm}^{-1}$ . The final spectra were convolved to a resolution of 15  $\text{cm}^{-1}$  assuming a sinc apparatus function. In our spectral range, the Jovian spectrum is a combination of thermal and reflected sunlight components. At 2450  $\text{cm}^{-1}$ , the Jupiter's spectrum is composed of one third of thermal radiation, whereas at 2530  $\text{cm}^{-1}$ , the reflected com-

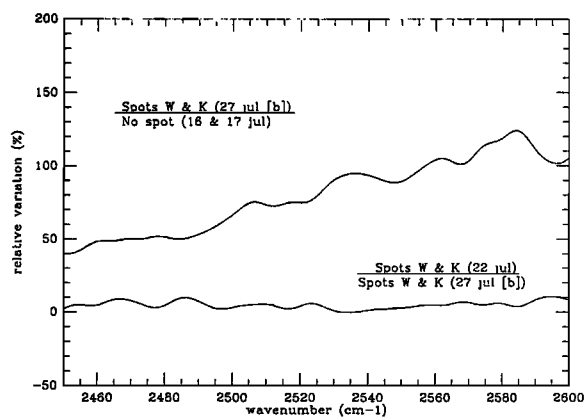


**Figure 2.** Ratio of a spectrum without spot divided by a spectrum corresponding to the W/K impact site. The increase from 2450 to 2600  $\text{cm}^{-1}$  is estimated to be due to the presence of a stratospheric haze formed by the comet collision. In addition, the ratio of two W+K spectra obtained on July 22 and July 27 is plotted. The haze appears very stable between the two dates.

ponent entirely dominates the spectrum. The thermal radiance originates from the troposphere of the planet while, in the absence of the comet impacts, the sunlight is reflected on the tropospheric  $\text{NH}_3$  cloud at  $\approx 0.5$  bar. The  $\text{NH}_3$  cloud single-scattering albedo was set to 0.12 in the study of the NEB. No albedo change was assumed between the northern and the southern hemisphere at the same absolute latitude of  $44^\circ$ . A transmission of 0.8 completes the description of the deep  $\text{NH}_3$  cloud. The presence of impacts has induced a stratospheric haze which has modified both the global shape and the spectral radiance of the spectrum. Hence, we have included such a haze in our model. Three parameters were accounted for in this modeling to obtain the best agreement between the computed and observed variation of the relative spectra: the haze albedo ( $a$ ), the transmission ( $t$ ) considered as a function of both the true transmission and the pure absorption by the particles, and the altitude of the corresponding reflecting layer ( $P$ ). In our study, several *a priori* assumptions have been made. The haze is assumed to be a thin cloud layer. The altitude of this haze is supposed to be between the 0.05 and 50 mbar pressure levels. Both W and K sites are assumed to be  $1.5 \times 1.5''$  circular spots at the central meridian.

The reason why the continuum of the spectra of impacts W/K is brighter than that of the undisturbed spectra is due to the simultaneous presence of strong intense  $\text{CH}_4$  absorption bands in our spectral range and of the stratospheric haze. The effect of a high stratospheric haze is to reflect and absorb photons in such a way that less photons are absorbed by methane at deeper pressure levels. Moreover, the increase of the variation of the relative spectra by a factor of 3 throughout our spectral range is directly due to the occurrence of more intense  $\text{CH}_4$  absorption bands at 2600 than at 2450  $\text{cm}^{-1}$ . As shown in Fig. 3, the albedo of the haze is strongly constrained by the data. The modeled spectra are compared with the observed spectra using the  $\chi^2(S)$  test. The reduced S is determined as the averaged

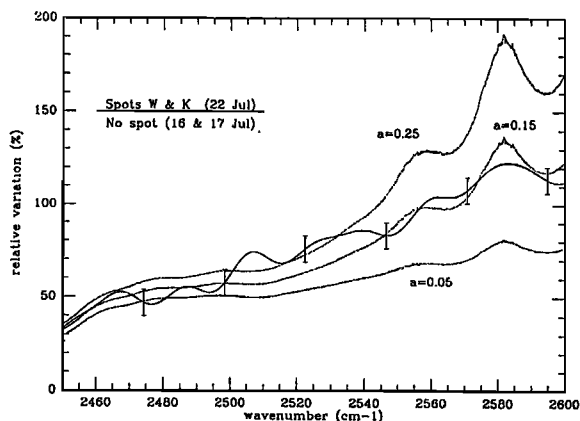


**Figure 3.** Model versus observations. The albedo of the haze is varied from 0.05 to 0.25. The sensitivity of the synthetic spectrum to the haze albedo is significant. The albedo is shown to be very close to 0.15 if the spot size is assumed to be  $3''$ .

**Table 1.** Stratospheric haze physical properties

Spectrum	$S_{min}$	Albedo at $3\sigma$	Pressure at $2\sigma$ (mb)	Best fit mb
22.07	1.5	0.13–0.17	0.05–5	$P=5/a=0.15$
27.07 [a]	2.7	0.13–0.20	–	$P=5/a=0.15$
27.07 [b]	1.9	0.08–0.15	0.5–50	$P=50/a=0.10$
27.07 [c]	3.8	0.13–0.18	–	$P=50/a=0.15$

dispersion between the observed and calculated relative variations of the spectra weighted by an error bar of 7%. This error bar was measured using two methods. The noise on each original spectrum was first measured outside of the band filter ( $\nu > 2750\text{cm}^{-1}$ ). It results in a 2–4% uncertainty on the spectrum depending on the spectral range. Equation (1) implies that the true uncertainty is twice that in each individual spectrum, i.e. 4–8%. The second method is obtained by measuring the dispersion between each relative spectra combination (each observed spectrum without spot is compared with each observed spectrum with the W/K spot). The resulting dispersion is again around 7%.

In the following, the results on the albedo are given at the  $3\sigma$  confidence level while those on the pressure level of the haze are at the  $2\sigma$  confidence level. The error bars are defined by the requirement that  $S$  be smaller than  $S_{min} \times \sqrt{1 + X^2/N}$  where  $X$  is the confidence level and the  $N$  number of points. The effective number of spectral points between 2450 and 2600  $\text{cm}^{-1}$  at a 15  $\text{cm}^{-1}$  resolution is 10. The limiting  $S$  is thus 1.38 and  $1.18 \times S_{min}$  at the  $3\sigma$  and  $2\sigma$  respectively. Table 1 summarizes the results concerning the physical characteristics of the haze and gives the best fit models for each observed spectrum. The most important parameter of the model is the albedo because the spectrum is dominated by the reflected sunlight component. The albedo of the haze is therefore  $0.14 \pm 0.01$ . The best fit model results in an altitude of the haze between 5 and 50 mb. Finally, the total transmission of the stratospheric haze is lower than 0.85. The extinction coefficient is therefore inferred to be lower than 0.15. Consequently, the assumption of a thin stratospheric haze in our calculations seems to be *a posteriori* validated. The possible sources of errors which can *a priori* strongly influence our results are:

- the thermal profile and its possible change,
- the albedo and transmission of the  $\text{NH}_3$  cloud,
- the size of the W/K sites.

Because we are forced to compare a spectrum obtained at a latitude of 44N to a spectrum located at 44S which could be modified by the impacts, we have to estimate what are the main differences between both latitudes in terms of thermal profile and  $\text{NH}_3$  cloud. Orton *et al.* (1991, 1994a) have intensively observed the stratospheric and tropospheric temperatures as a function of time and latitude. They have shown that a small difference of a few degrees was suggested between 44S and 44N depending on the altitude level. This hemispheric asymmetry has been taken into account in our calculations by changing the standard thermal profile by the

corresponding temperature shift. It results only in a one percent level variation in the spectral radiance of the without spot spectrum. The temperature asymmetry can thus be neglected for our purpose. In addition to this hemispheric “standard” variation, another uncertainty related to the impacts themselves should be analyzed. From broadband millimeter wavelength observations, Gurwell *et al.* (1994) have seen no obvious impact effect on the temperature brightness at a pressure level of 0.8 bar. At higher pressure level, from infrared observations, Orton *et al.* (1994b) have detected some temperature changes in the troposphere of a few degrees at a level of 400 mb at the impact sites for several days. Moreover, Billebaud *et al.* (1994) derived a variation of 2.5–4.5 K at a level of at least 30 mb from 8  $\mu\text{m}$  observations of W and K impacts. Finally, Lellouch *et al.* (1994), Marten *et al.* (1994b) derived indirectly from millimeter and submillimeter heterodyne spectroscopy a strong increase of the temperature (several tens of K) in the stratosphere above at least a few mb for several days. This “abnormal” thermal profile was observed to vary from day to day, providing emission lines of CO, CS and HCN during the impacts and absorption lines after a few weeks. Both tropospheric and stratospheric changes were tested in our calculations by including the new thermal profile of the impact sites. Again such a modification is not important in our study because most of the thermal component ( $\nu < 2530\text{cm}^{-1}$ ) is coming from the deeper pressure levels of the planet where the temperature profile is very little modified.

Conversely, a strong hemispheric asymmetry of the  $\text{NH}_3$  cloud albedo and transmission directly results in a significant difference of the spectral radiance of the Jovian spectrum. Many calculations were thus performed to estimate this uncertainty. The reflected layer of the ammonia cloud was fixed at  $\approx 0.5$  bar. The first step of these calculations was to try to fit the relative variation (Fig. 2) by changing only the characteristics of the  $\text{NH}_3$  cloud in the Southern hemisphere not taking into account the stratospheric haze. The best fit is obtained by increasing the albedo of the  $\text{NH}_3$  cloud by a factor of  $\approx 2$ . In this case, the fit between the observed and calculated relative variation of the Jovian spectrum is however very bad. A  $\chi^2$  test will give a  $S$  of  $\approx 7$ , as compared to a typical  $S$  of 2 if the stratospheric haze was only taken into account. Nevertheless, the uncertainty due to this  $\text{NH}_3$  cloud produces an uncertainty in the estimate of the albedo of the stratospheric haze within a factor of 2.

Griffith *et al.* (1994) estimated the size of the fragments W and K site as a unique spot between 2–4” in diameter. This size has not strongly evolved 10 days after the last impact. If the W/K site is assumed to be a 4” circular spot rather than twice 1.5” spots, the albedo of the haze will change by 10 %.

## Discussion

The altitude and thickness of the haze are a key problem for the understanding of the collision pro-

Table 2. Spectral properties of the haze particles

Wavelength	Optical depth	Reference	$n_i$	$\omega_0$
0.27 $\mu\text{m}$	12	Noll <i>et al</i> (1994)	0.02	0.76
0.89 $\mu\text{m}$	2.4	West <i>et al</i> (1994)	0.006	0.97
2.14 $\mu\text{m}$	0.1	Baines <i>et al</i> (1994)	0.05	0.53
3.9 $\mu\text{m}$	0.07–0.15	This paper	0.01	0.4
8–12 $\mu\text{m}$	0.01	Gierasch <i>et al</i> (1994)	0.01	0.01

cesses. From our data, the altitude of the haze has been marginally constrained below 5 mb, but we do not claim this pressure limit is a firm result. From near infrared data (1–2.5  $\mu\text{m}$ ), DePoy *et al.* (1994) have suggested a haze altitude around 1 mb, strongly depending on the impact site. At 2.3  $\mu\text{m}$ , the haze altitude has been derived to be around 10 mb (Gierasch *et al.*). West *et al.* (1994) have finally proposed an extended aerosol layer stretched between at least 200 mb and a few mb.

Concerning the low opacity of the haze layer at mid infrared wavelengths after the impacts, it could be consistent with a sedimentation of the dust particles coming from the high stratosphere to the deeper pressure level. The high stability from July 22 to July 27 demonstrates that the evolution of the haze is nevertheless very slow. Until today, this haze is still observed. Even if its opacity is slowly decreasing and a simultaneous complex spatial extension is occurring, particles seem to be still present in the stratosphere.

Assuming a unique size for the haze particles, the transmission  $t$  is related to the extinction coefficient  $\gamma$  through the usual Mie formulae assuming spherical particles:

$$\gamma = -\frac{\ln t}{l} = \pi r^2 Q_{ext} N \quad (2)$$

where  $r$  is the radius of the particles,  $N$  the number density of particles, and  $Q_{ext}$  the efficiency factor for extinction. The optical depth  $\tau$  is the product  $\gamma l$ , where  $l$  is the thickness of the haze. Since  $t$  is larger than 0.85,  $\tau$  is lower than 0.15. Equation 2 is true for optical depths lower than 0.2 where multiple scattering can be neglected. In the following, we have assumed that  $r=0.25 \mu\text{m}$  as proposed by Baines *et al.* (1994) for calculating the single scattering albedo  $\omega_0$  of the particles in the Mie approximation. For large optical depths, the imaginary refractive index given by West *et al.* (1994) at 0.27 and 0.89  $\mu\text{m}$  enables direct calculation of  $\omega_0$ . From 2.14  $\mu\text{m}$  to 10  $\mu\text{m}$ , the optical depth is low enough to apply equation (2). Knowing the efficiency factor for extinction  $Q_{ext}$ , we can calculate both the efficiency factor for absorption  $Q_{abs}$  and efficiency factor for scattering  $Q_{sca}$  and the imaginary refractive index at each wavelength. The results are reported in Table 2. At 3.9  $\mu\text{m}$ ,  $\omega_0$  is around 0.4. The particles are therefore significantly absorbing in the mid infrared. The number density of the particles over the W/K site

is  $\approx 4 \cdot 10^9 \text{ cm}^{-2}$ . They should play an important role in the thermal balance over the impact sites.

**Acknowledgments.** The authors are very grateful to Bruno Bésard for fruitful discussions and wish to thank Block Engineering - Diamond Electro-Optics company for cooperative efforts.

## References

- Baines, K.H., *et al.* The Effect of SL9 on Jupiter's Vertical Aerosol Structure: Results from IRTF Near-Infrared Imaging. *Bull. Amer. Astron. Soc.*, **26**, 26, 1994.
- Billebaud, F., *et al.* 10  $\mu\text{m}$  Mapping of Jupiter on the CFHT after the Impacts of Comet P/Shoemaker-Levy 9. *Submitted to Geophys. Res. Lett.*, this issue, 1994.
- DePoy, D.L., *et al.* Near-IR Observations of the Comet Crash from Cerro Tololo. *Bull. Amer. Astron. Soc.*, **26**, 27, 1994.
- Gierasch, P., *et al.* A Physical Interpretation of the SL-9 Impacts Observed from Palomar. *Bull. Amer. Astron. Soc.*, **26**, 20, 1994.
- Griffith, C., *et al.* Mid-IR spectroscopy and Ammonia Images of K Impact Site. *Bull. Amer. Astron. Soc.*, **26**, 19, 1994.
- Gurwell, M.A., *et al.* Millimeter Imaging of the Comet P/Shoemaker-Levy 9 Impacts on Jupiter. *Bull. Americ. Astron. Soc.*, **26**, 18, 1994.
- Lellouch, E., *et al.* The collision of comet P/Shoemaker-Levy 9 with Jupiter: chemical and thermal constraints from detection of CO, CS and OCS. *Submitted to Nature*, 1994.
- Marten, A., *et al.* Four micron high-resolution spectra of Jupiter in the North Equatorial Belt:  $\text{H}_3^+$  emissions and the  $^{12}\text{C}/^{13}\text{C}$  ratio. *Planet. Space Sci.*, **42**, 391–399, 1994a.
- Marten, A., *et al.* New heterodyne millimeter observations of Jupiter performed after the collision of comet SL-9 with the planet. *Bull. Amer. Astron. Soc.*, **26**, 24, 1994b.
- Orton, G.S., *et al.* Thermal Maps of Jupiter: Spatial Organization and Time Dependence of Stratospheric Temperatures, 1980 to 1990. *Science*, **252**, 537–542, 1991.
- Orton, G.S., *et al.* Zonal-mean temperature structure, composition and cloud properties of Jupiter in 1989 October from high resolution spectroscopic thermal imaging. *Bull. Amer. Astron. Soc.*, **24**, 1041, 1992.
- Orton, G.S., *et al.* Thermal Maps of Jupiter: Spatial Organization and Time Dependence of Tropospheric Temperatures, 1980 to 1993. *Submitted to Science*, 1994a.
- Orton, G.S., *et al.* The NASA Infrared Telescope Facility Investigation of Comet Shoemaker-Levy 9 and its Collision with Jupiter: Preliminary Results. *submitted to Science*, 1994b.
- West, R.A., *et al.* Wide-Field/Planetary Camera 2 Observations of Jupiter's Stratospheric Haze and Ammonia Cloud: Post Impact. *Bull. Americ. Astron. Soc.*, **26**, 25, 1994.

J. Rosenqvist, DESPA, Observatoire de Paris-Meudon, F-92195 Meudon, France

(received December 10, 1994; revised February 1, 1995; accepted February, 1995.)